

**Case-Specific Parametric Analysis as Research-Directing Tool  
for Analysis and Design of GFRP-RC Structures**

Marco Rossini, Eleonora Bruschi, Fabio Matta, Carlo Poggi, Antonio Nanni

**Synopsis:** This paper presents a parametric analysis of the ACI 440 and AASHTO algorithms governing the flexural design of a one-way concrete member internally reinforced with glass fiber-reinforced polymer (GFRP) bars. The influence of specific design parameters on the amount of reinforcement is investigated. The aim is to understand which variables and requirements govern the design, and how they affect the required amount of reinforcement. The member is the reinforced concrete (RC) pile cap of the Halls River Bridge (Homosassa, FL), which is representative of a large-size GFRP-RC member in short-span bridges. Cyclic fatigue and creep rupture are identified as mechanisms governing the design, and the influence of four critical parameters on the required reinforcement is assessed. Salient analysis and design implications are discussed with respect to creep and fatigue rupture stress limits, minimum amount of flexural reinforcement, and applicable strength reduction factors. The outcomes of the parametric analysis highlight an untapped potential to significantly reduce the required amount of reinforcement, and offer a perspective on research areas to prioritize to advance the development of rational design algorithms.

**Keywords:** concrete; design; flexure; GFRP bars; parametric analysis; safety factors; standards.

**Marco Rossini** is a PhD student in the Department of Civil, Architectural, and Environmental Engineering at the University of Miami, FL. He received his M.S. in Structural Engineering and his B.S. in Civil Engineering from the Politecnico di Milano, Italy. His research interests include corrosion-resistant internal reinforcement for concrete, and the development of rational design methods.

**Eleonora Bruschi** is a M.S. student in Structural Engineering at the Politecnico di Milano, Italy. She received her B.S. in Civil Engineering from the same institution. Her research interests include corrosion-resistant internal reinforcement for concrete, and the development of rational design methods.

**Fabio Matta** is an Associate Professor in the Department of Civil and Environmental Engineering at the University of South Carolina, Columbia. He serves as voting member of ACI Committee 241 (Nanotechnology of Concrete) and 446 (Fracture Mechanics of Concrete), and associate member of ACI Committee 440 (Fiber Reinforced Polymer Reinforcement). His research interests include sustainable and durable material systems for the construction and rehabilitation of concrete structures.

**Carlo Poggi** is Full Professor in Structural Analysis in the School of Building Engineering at Politecnico of Milano and is member of the Department ABC of Architecture, Built environment and Construction Engineering. His research interests include innovative systems for the construction and rehabilitation of structures.

**Antonio Nanni**, F.ACI, F.ASCE, is the Inaugural Senior Scholar, Professor and Chair, in the Department of Civil, Architectural, and Environmental Engineering at the University of Miami, FL. He serves as Chair of ACI Committee 549 and Subcommittee 562-E. He serves as voting member of ACI Committees 437, 440, and 562. His research interests include construction materials and their structural performance and field application.

#### LIST OF SYMBOLS

|                   |                 |  |
|-------------------|-----------------|--|
| #                 | -               | GFRP bar number.   |
| $a_f$             | in <sup>2</sup> | Nominal cross-sectional area of GFRP bar.                        |
| $b$               | in.             | Width of the concrete cross section.                             |
| $A_{fL}$          | in <sup>2</sup> | Area of GFRP longitudinal reinforcement.                         |
| $A_{f,min}$       | in <sup>2</sup> | Minimum area of GFRP longitudinal reinforcement.                 |
| $c_c$             | in.             | Concrete clear cover.  |
| $C_c$             | -               | Creep rupture reduction factor.                                  |
| $C_E$             | -               | Environmental reduction factor.                                  |
| $C_f$             | -               | Cyclic fatigue reduction factor.                                 |
| $d$               | in.             | Effective depth of the concrete cross section.                   |
| $d_b$             | in.             | Nominal diameter of the GFRP bar.                                |
| $E$               | -               | Effectiveness ratio, as defined in Eq. 6.                        |
| $E_f$             | ksi             | Design modulus of elasticity of GFRP bar.                        |
| $f_c'$            | ksi             | Specified compressive strength of concrete.                      |
| $f_{fc}$          | ksi             | Creep rupture strength of GFRP bar.                              |
| $f_{ff}$          | ksi             | Cyclic fatigue rupture strength of GFRP bar.                     |
| $f_{fu}$          | ksi             | Design strength of GFRP bar.                                     |
| $f_{fu}^*$        | ksi             | Guaranteed strength of GFRP bar.                                 |
| $M_{cr}$          | kip-ft          | Cracking moment.   |
| $M_f^+$           | kip-ft          | Fatigue I combination positive bending moment demand.            |
| $M_n$             | kip-ft          | Nominal moment capacity.   |
| $M_r$             | kip-ft          | Factored moment capacity.  |
| $M_s^+$           | kip-ft          | Service I combination positive bending moment demand.            |
| $M_{s+f}^+$       | kip-ft          | Combined Service I and Fatigue I positive bending moment demand. |
| $M_u^-$           | kip-ft          | Strength negative bending moment demand.                         |
| $M_u^+$           | kip-ft          | Strength positive bending moment demand.                         |
| $V_u$             | kip             | Strength shear demand.   |
| $\epsilon_{fu}$   | in./in.         | Design rupture strain of GFRP bar.                               |
| $\epsilon_{fu}^*$ | in./in.         | Guaranteed rupture strain of GFRP bar.                           |
| $\phi$            | -               | Strength reduction factor for flexure.                           |

|             |                             |  |
|-------------|-----------------------------|--|
| $\phi_c$    | -                           | Strength reduction factor for flexure, compression-controlled. |
| $\phi_t$    | -                           | Strength reduction factor for flexure, tension-controlled.     |
| $\rho_f$    | $\text{in}^2 / \text{in}^2$ | Reinforcement ratio.   |
| $\rho_{fb}$ | $\text{in}^2 / \text{in}^2$ | Reinforcement ratio for the balanced section.                  |

## INTRODUCTION

The first generation of analysis and design provisions succeeded in addressing the behavior of glass fiber-reinforced polymer (GFRP) reinforced concrete (RC) structures, and the differences with respect to conventional steel RC structures (Nanni, 1999). However, the availability of a limited experimental database at that time called for the introduction of relatively severe safety factors (Jawaheri & Nanni, 2013). This limitation prevents one from taking full advantage of the efficiency and economical appeal of GFRP bars, as highlighted by the ever-growing knowledge of and experience with GFRP-RC structures (Nanni & Faza, 2002).

Numerous studies contributed to update the first-generation design guides, sometimes allowing for a relaxation of originally over-conservative assumptions, thereby allowing for a more efficient use of GFRP bars. More research is constantly needed to make these design provisions more rationale and address the growing demand for more sustainable solutions with limited life-cycle costs. However, what should be the focus of further research is a question that is not addressed in a systematic fashion. As a result, there may be an important margin of improvement based on the prioritization of higher-impact research themes, and the deployment of the available economical and intellectual resources.

This study is a first attempt to address what would be a more efficient employment for such resources. To this end, a parametric analysis of the ACI (2015) and AASHTO (2009) algorithms governing the flexural design of a GFRP-RC element was performed. This analysis enables one to quantify the influence of each design requirement and safety factor (including environmental reduction factor,  $C_E$ , and strength reduction factor,  $\phi$ ) on the design outcome (i.e., required amount of reinforcement).

## METHODOLOGY

The study focuses on the RC pile cap of the Halls River Bridge (Homosassa, FL). The cross section of the bridge is illustrated in Figure 1, where the pile cap is highlighted and the design section for positive bending moment (AA) is indicated. The cross section and reinforcement layout of the pile cap is illustrated in Figure 2. Here, the influence of relevant design parameters on the required amount of reinforcement is investigated. Results are also discussed in terms of potential savings on the required amount of reinforcement.

The moment and shear demands were as provided by the Florida DOT. The values reported herein are typical of short-span vehicular bridges. The positive bending moment, negative bending moment, and shear force demand are  $M_u^+ = 424$  kip-ft (575 kN-m),  $M_u^- = 281$  kip-ft (381 kN-m), and  $V_u = 185$  kip (823 kN), respectively. The positive bending moment demand for Service I load combination (AASHTO, 2014) is  $M_s^+ = 280$  kip-ft (380 kN-m) while for Fatigue I load combination the demand is  $M_f^+ = 81$  kip-ft (110 kN-m). Flexural design for positive moments is considered where failure is controlled by FRP rupture.

The design parameters are: GFRP longitudinal bar size (#8,  $d_b = 25$  mm) and nominal area ( $a_f = 0.79$  in<sup>2</sup> or 510 mm<sup>2</sup>), GFRP stirrup size (#5,  $d_b = 16$  mm) and nominal area ( $a_f = 0.31$  in<sup>2</sup> or 200 mm<sup>2</sup>), GFRP bars elastic modulus ( $E_f = 6,500$  ksi or 45 GPa), GFRP longitudinal GFRP bar guaranteed strength and ultimate strain ( $f_{fu}^* = 85.63$  ksi or 590 MPa,  $\varepsilon_{fu}^* = 0.013$ ), specified concrete cylinder compressive strength ( $f_c' = 6.5$  ksi or 45 MPa) and clear cover ( $c_c = 3$  in. or 76 mm).

In addition, the parameters whose variation was considered in this study along with their original value are listed hereinafter: environmental reduction factor ( $C_E = 0.7$ ), moment capacity reduction factor for tension-controlled sections ( $\phi_t = 0.55$ ), creep rupture reduction factor ( $C_C = 0.2$ ) and cyclic fatigue reduction factor ( $C_f = 0.2$ ).

Each parametric curve is constructed by calculating the minimum amount of #8 GFRP bars, expressed in terms of cross sectional area,  $A_{fL}$ , that satisfies the specific design requirement: moment capacity, minimum reinforcement, creep rupture and fatigue limits. The design for positive moment capacity based on ACI (2015) and AASHTO (2009) resulted in 16 #8 bars, for a total area of 12.53 in<sup>2</sup> (8,084 mm<sup>2</sup>) as showed in Figure 2.

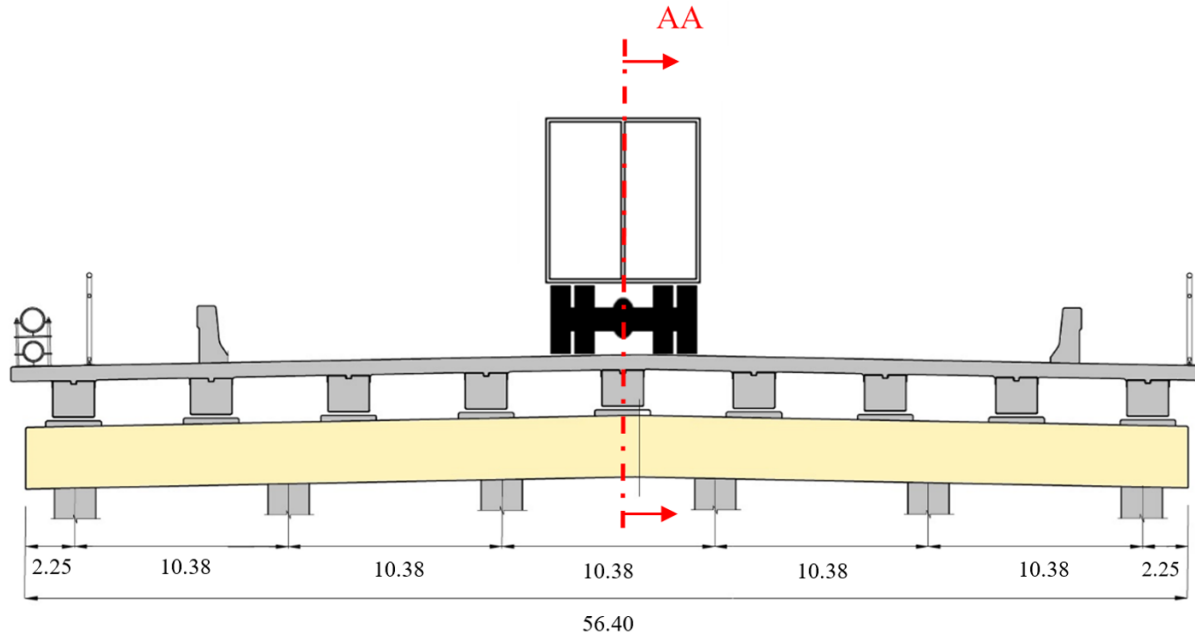


**Figure 1** – Transverse cross section of bridge superstructure with reference cross section (AA) of pile cap. Dimensions in ft. (1 ft. = 0.3048 m).

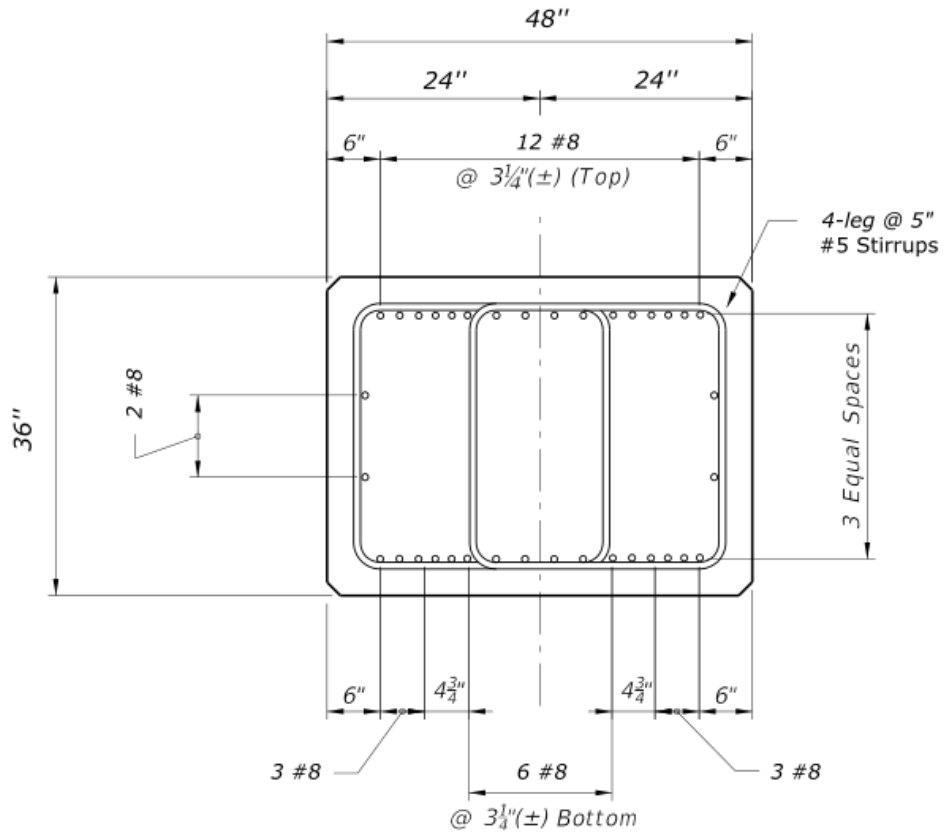


**Figure 2** – Cross section geometry and reinforcement layout of pile cap (section AA in Figure 1). Dimensions in in. (1 in. = 25.4 mm).

The ACI (2015) recommendations generally coincide with the AASHTO (2009) provisions, despite the two guides use different units: the AASHTO customary-unit (ksi, kip) convention is used hereinafter, and ACI algorithms are converted accordingly.

### **DESIGN PARAMETERS**

Four critical design parameters are considered for the parametric analysis: moment capacity reduction factor ( $\phi$ ) affecting the design moment capacity; environmental factor ( $C_E$ ) accounting for strength degradation in GFRP-RC members operating in aggressive environments; creep rupture and fatigue GFRP reduction factors ( $C_c$  and  $C_f$ ).

#### **Moment capacity reduction factor**

The strength reduction factor  $\phi$  accounts for the stochastic variation of the materials resistance, not covered by the definition of a guaranteed strength in the case of GFRP, as well as for the uncertainties intrinsic in the analysis model. Conversely, the stochastic nature of the load factors is not accounted for in this “safety” factor, whereas it is accounted for when using the AASHTO load factors (AASHTO, 2014). Both ACI (2015) and AASHTO (2009) adopt the following values:

$$\phi = \begin{cases} 0.55 & \rho_f \leq \rho_{fb} \\ 0.3 + 0.25 \frac{\rho_f}{\rho_{fb}} & \rho_{fb} < \rho_f < 1.4\rho_{fb} \\ 0.65 & \rho_f \geq 1.4\rho_{fb} \end{cases} \quad (1)$$

In the original version of the ACI 440 guidelines (ACI, 2001), a smaller strength reduction factor for tension-controlled failure compared to compression-controlled failure was assumed. The goal was to account for the higher variability of moment capacity associated with FRP rupture, and to account for the brittle failure of the FRP reinforcement as opposed to the softening (quasi-brittle) behavior of concrete (Nanni 1993, Nanni & Faza 2002). At the current state of knowledge, such a conservative approach seems to offer margins of improvement.

For what concerns provisions harmonization, it is noted that AASHTO (2014) specifies a 0.75 strength reduction factor for compression-controlled failure in steel-RC members, in contrast with the 0.65 in ACI (2014, 2015) and AASHTO (2009).

Looking at international FRP design guides and focusing on tension-controlled failure, the Japanese recommendations (JSCE, 1997) suggest a strength reduction factor variable between 0.59 and 0.67. The Italian guide (CNR, 2007) suggests 0.67, and the Canadian code (CSA, 2014) specifies 0.65, similar to ACI (2015) and AASHTO (2009).

Several studies have investigated the issue from different perspectives and adopting various reliability models. For example, Benmokrane et al. (1996) suggest a value of 0.75, while Jawaheri & Nanni (2013) suggest a 0.7 reduction factor for both tension- and compression-controlled failure. A variation from 0.55 to 0.75 for tension-controlled failure is considered in the parametric analysis in this study.

The strength reduction factor only affects the nominal moment capacity. When failure occurs because of rupture of the GFRP reinforcement, as for the pile cap member analyzed herein, the concrete rectangular stress block approach is not applicable since the ultimate concrete strain  $\epsilon_{cu} = 0.003$  is not attained. For this case, both ACI (2015) and AASHTO (2009) provide a simplified and conservative approach to compute the nominal moment capacity.

#### **Environmental reduction factor**

Both ACI (2015) and AASHTO (2009) highlight the need to reduce the guaranteed tensile strength and the guaranteed rupture strain to be used to determine the nominal moment capacity, in order to account for long-term environmental effects. This is accomplished by means of an environmental reduction factor,  $C_E$ , as follows:

$$f_{fu} = C_E \cdot f_{fu}^* \quad (2)$$

$$\epsilon_{fu} = C_E \cdot \epsilon_{fu}^* \quad (3)$$

The environmental reduction factor varies depending on the type of fiber and exposure condition (Table 1). These values are believed to be conservative and depend on the experienced durability performances of each fiber type. Temperature effects are accounted for in the  $C_E$  values; however, FRP bars should not be used in environments with service temperatures greater than the glass transition temperature of the resin ( $T_g$ ) minus a preset temperature buffer (e.g., 18°F or 10°C).

ACI (2015) expresses the expectation that, with continued research,  $C_E$  values will become more reflective of the actual environmental performance. In the parametric analysis, an environmental reduction factor in the range 0.70-0.95 is considered.

| Exposure condition                        | Fiber  | Environmental reduction factor, $C_E$ |
|---|--------|---------------------------------------|
| Concrete not exposed to earth and weather | Carbon | 1.0                                   |
|   | Glass  | 0.8                                   |
|   | Aramid | 0.9                                   |
| Concrete exposed to earth and weather     | Carbon | 0.9                                   |
|   | Glass  | 0.7                                   |
|   | Aramid | 0.8                                   |

**Table 1** – Environmental reduction factor per ACI 440, Table 6.2 (ACI, 2015)

**Creep rupture reduction factor**

Glass is well known to undergo static fatigue under sustained load (Wiederhorn & Boltz, 1970), and polymeric matrices are expected to experience creep deformation over time (Hugo et al., 1993). The two phenomena are of different mechanical nature, and concur in affecting the static fatigue life of GFRP reinforcement. To this end, stresses under sustained load are limited to a fraction of the instantaneous rupture strength. The nomenclature “creep rupture reduction factor” and the notation “ $C_c$ ” are herein proposed for clarity and separation from cyclic fatigue.

This factor is set to 20% of the design tensile strength in both the ACI (2015) guidelines (Table 2) and the AASHTO (2009) specifications. However, greater values are found in international provisions: 25% is specified by CSA (2014), and 30% by CNR (2007). It is noted that the  $C_c$  limit is applied to the design strength, which has already been reduced by means of the environmental reduction factor; for example, for  $C_E = 0.7$  and  $C_c = 0.2$ , the stress limit is 14% of the GFRP guaranteed tensile strength, which might be overly penalizing. In the parametric analysis, a reduction factor in the range 0.2-0.5 is considered.

Stresses produced by service loads [ $M_s^+ = 280$  kip-ft or 380 kN-m for Service I load combination per AASHTO (2014)] can be computed via elastic analysis and should be limited to 20% of the design load. Considering the entire service load permanently applied to the structure (AASHTO, 2009) appears be overconservative, and more research is needed to gain further insight.

| Fiber type                              | GFRP          | AFRP          | CFRP          |
|---|---------------|---------------|---------------|
| Creep rupture stress limit $f_{fs,sus}$ | 0.20 $f_{fu}$ | 0.30 $f_{fu}$ | 0.55 $f_{fu}$ |

**Table 2** – Creep rupture stress limits per ACI 440, Table 7.4.1 (ACI, 2015).

**Cyclic fatigue reduction factor**

According to both ACI (2015) and AASHTO (2009), the same limit defined for creep rupture applies also as cyclic fatigue stress limit. It is expected that further research in the fatigue behavior of GFRP would lead to a better characterization of the material and a cyclic-load-focused design approach equivalent to what AASHTO (2014) specifies for steel-RC members. The independent nomenclature “cyclic fatigue reduction factor” and the notation “ $C_f$ ” are here proposed for clarity and separation from creep rupture. A variation from 0.2 to 0.5 is considered.

Stresses in a fatigue cycle under service loads can be computed via an elastic analysis. Existing US provisions present discrepancies in defining the load combination to consider for fatigue analysis, two alternatives can be identified:

1. AASHTO (2009) refers to the Fatigue I load combination (AASHTO 2014). This combination does not account for the permanent load component and is typically less demanding than the Service I load combination referred for creep rupture verification ( $M_f^+ = 81$  kip-ft or 110 kN-m). Such approach comes with the assumption that the cyclic fatigue rupture stress for GFRP bars is not affected by sustained stresses due to permanent loads. More research is needed to verify this assumption.
2. ACI (2015) recommends considering all sustained load in addition to the maximum load acting during a fatigue cycle. Translating the provision into AASHTO language may entail combining the sustained load in Service I plus the fluctuating load from Fatigue I load combinations (AASHTO, 2014), resulting in a more demanding condition than the one used for creep rupture verification ( $M_{s+f}^+ = 361$  kip-ft or 489 kN-m). This approach lumps static and cyclic fatigue demand, thereby coupling the two phenomena. This assumption of a fully coupled behavior, with the entire service load permanently applied to the structure, appears to be overconservative especially when compared to the CSA (2014) provisions. Still, this approach guarantees consistency with ACI (2015) approach and compliance with AASHTO (2009) provisions.

The discrepancy between the AASHTO (2014) and ACI (2015) demands can be explained looking at the different approaches adopted for fatigue design. While ACI (2015) recommends limiting the total load resisted by the member, AASHTO (2014) traditionally imposes a limit on the variation of load the structure experiences over a fatigue cycle, disregarding the permanent component.

### DESIGN REQUIREMENTS

Both ACI (2015) and AASHTO (2009) require that design fulfill a range of different requirements, for which the parameters considered in this study play an important role. The study focuses on strength-related requirements, either short- or long-term (ultimate moment capacity, creep rupture, cyclic fatigue). Service-related counterparts (crack-opening, temperature and shrinkage reinforcement, deflection, concrete admissible stress) are left aside although, in some instances, they may control design.

The minimum reinforcement requirement will be considered as a baseline for comparison. Such requirement will be expressed as an explicit ratio of the nominal moment capacity to the cracking moment (Eq. 4), following the unified approach proposed by Gamble (2017) and for consistency with AASHTO (2014). Imposing a 1.6 ratio results in a requirement analogous to the traditional ACI (2015) equation (Eq. 5):

$$\frac{\phi M_n}{M_{cr}} \geq 1.6 \tag{4}$$

$$A_{f,min} = 0.16 \frac{\sqrt{f_c'}}{f_{fu}} (bd) \geq \frac{0.33}{f_{fu}} (bd) \tag{5}$$

### RESULTS AND DISCUSSION

The present required reinforcement for the pile cap in HRB consists in 16 #8 GFRP bars, for a total area of 12.53 in<sup>2</sup>, computed per ACI (2015) recommendations. The design is controlled by the fatigue requirement.

For each parameter, the range considered in the analysis, the design requirements affected, and the potential reduction in required reinforcement, are summarized in Table 3. The “x” in a given cell of the table indicates correlation between parameter and requirement.

| Parameters | Range       | Moment capacity | Minimum reinforcement | Creep rupture | Cyclic fatigue | $A_{fL}$ potential reduction |
|------------|-------------|-----------------|-----------------------|---------------|----------------|------------------------------|
| $\phi$     | 0.55 – 0.75 | x               | x                     |               |                | 27%                          |
| $C_E$      | 0.70 – 0.95 | x               | x                     | x             | x              | 27%                          |
| $C_C$      | 0.2 – 0.5   |                 |                       | x             |                | 61%                          |
| $C_f$      | 0.2 – 0.5   |                 |                       |               | x              | 61%                          |

**Table 3** – Varied parameters and their effects in terms of reinforcement savings.

#### Requirements over single parameter variation

Figure 3 shows the influence of each parameter on the required amount of reinforcement. The design demand is represented in terms of required area of longitudinal reinforcement. For each parameter, all design equations are

plotted as a function of the selected range (Table 3). The results presented in Figure 3 are case-dependent but the trend of the curves is indicative in general.

For members with a large cross-section, as in the case of the pile cap, design is typically not governed by the moment capacity requirement. Therefore, varying the strength reduction factor,  $\phi$ , would have little influence on the final design, as illustrated in Figure 3a. The potential 27% reduction reported in Table 3 may only be achieved in members where the design is strength-controlled.

The environmental reduction factor,  $C_E$ , affects the required minimum amount of reinforcement, creep rupture, fatigue as well as strength design, as shown in Figure 3b. Any relaxation stemming from research as well as improved constituent materials would result in reductions per Table 3.

The severe demand in terms of static fatigue load and the limitation on creep rupture stress limit (based on  $C_c$ ), make this a governing requirement over strength. The definition of a less stringent creep rupture reduction factor (Figure 3c) based on more research on GFRP bars behavior, would result in significant reductions in reinforcement area (Table 3).

Similarly, the cyclic fatigue stress limit (based on  $C_f$ ) always controls over the strength requirement (Figure 3) and, in reason of a higher demand with respect to creep rupture, cyclic fatigue controls the design of the member. Also in this case, the definition of a less stringent reduction factor (Figure 3d), would result in significant reductions in reinforcement area (Table 3), along with a switch in the governing design requirements.

Any intervention on creep or fatigue limits would be effective as long as the minimum reinforcement does not become the governing design requirement, as marked by the curve intersections in Figure 3c and Figure 3d.

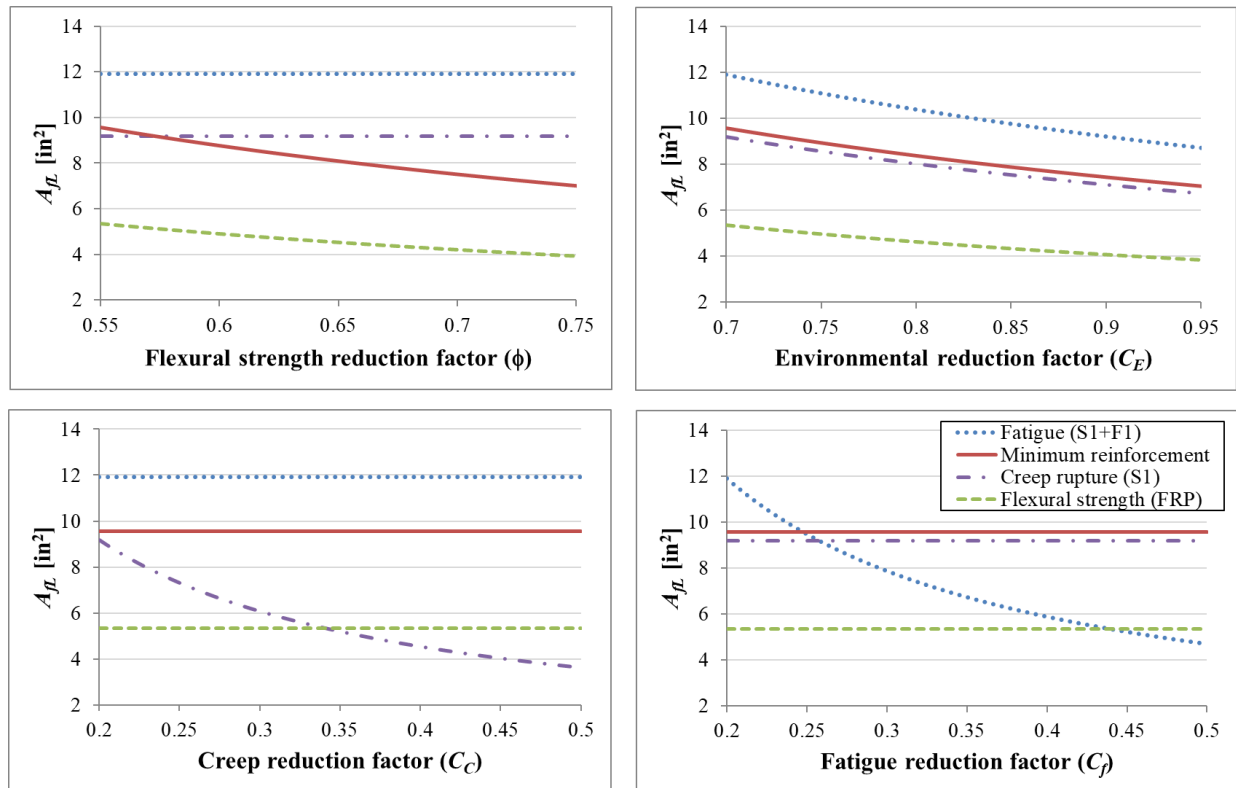


Figure 3 – Required area of reinforcement as function of analysis parameters (1 in<sup>2</sup> = 645 mm<sup>2</sup>).

**Interplay of parameters**

Assuming the same percentage increment on each parameter allows to plot in a single diagram multiple curves, all expression of the same design equation, as a function of the increment of the different parameters. These non-



dimensional plots (Figure 4) allow to compare the influence of each parameter has on a particular design requirement, instead of comparing the behavior of different design requirements as a function of the same parameter.

When the dependency on different parameters is similar, the curves overlap, as in the case of the environmental reduction factor, creep rupture reduction factor, and fatigue reduction factor in Figure 4c and Figure 4d. In such cases, the same style is applied to the overlapping lines, for clarity.

Each design equation shows an almost linear dependency on the increment of each of the affecting parameters. The slope of each curve can be taken as a measure of the effectiveness that, acting on each design parameters, has on the design outcome. The effectiveness parameter ( $E$ ) is dimensionless and unbounded: the higher, the more effective. Table 4 sums up the potential effectiveness that the variation of each parameter (one per each column) has on each design requirement (one per each row).

$$E = \tan \left[ \frac{\Delta (A_{FL} \text{ Savings})}{\Delta (\text{Parameter Increment})} \right] \quad (6)$$

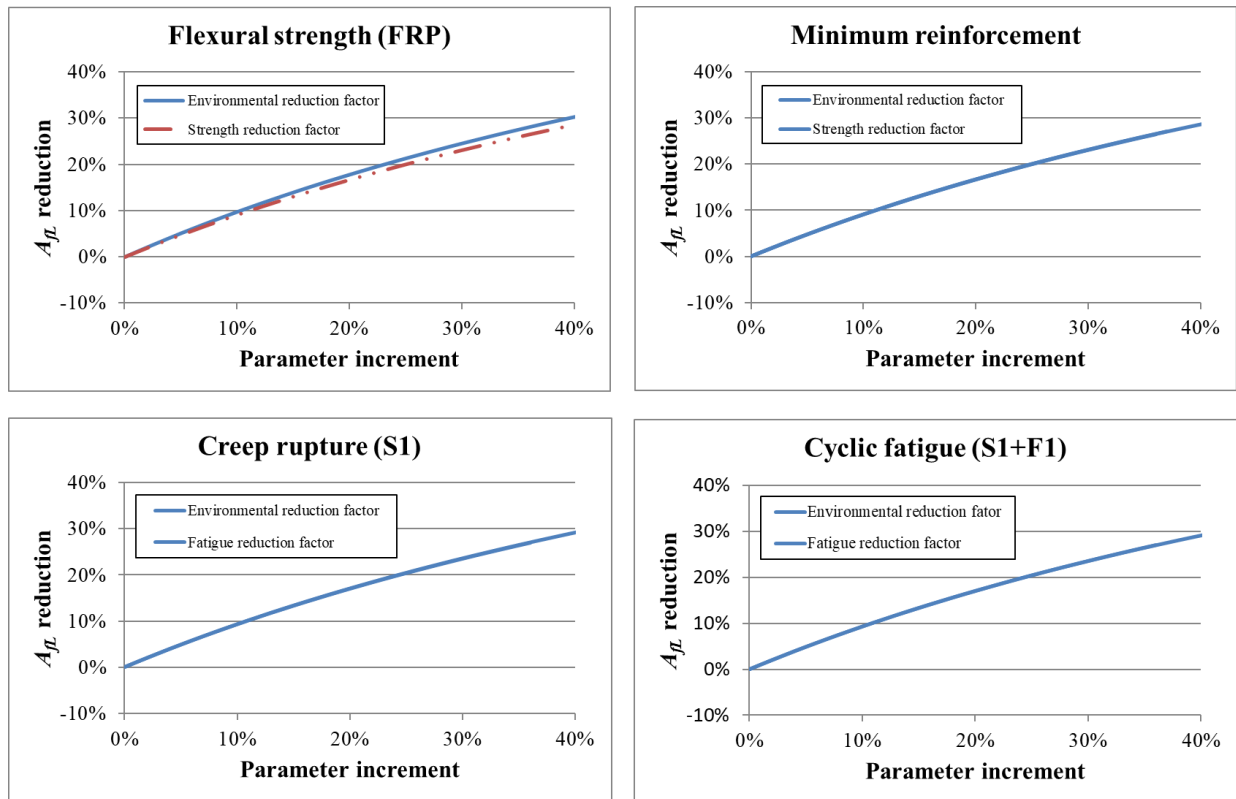


**Figure 4** – Requirement dependency on various affecting parameters, plotted in the same diagram.

| Design requirements    | $E(\phi)$ | $E(C_E)$ | $E(C_C)$ | $E(C_f)$ |
|------------------------|-----------|----------|----------|----------|
| Moment capacity (FRP)  | 0.85      | 0.93     | -        | -        |
| Minimum reinforcement  | 0.85      | 0.85     | -        | -        |
| Creep rupture (S1)     | -         | 0.88     | 0.88     | -        |
| Cyclic fatigue (S1+C1) | -         | 0.88     | -        | 0.88     |

**Table 4** – Effectiveness related to each parameter variation on each design equation.

### IMPLICATIONS FOR FUTURE RESEARCH

Figure 4 and Table 4 show how the variation of each parameter has almost the same influence on each affected equation. Once the priorities are set in terms of controlling design requirement, the parameter to investigate shall be selected depending on the actual research feasibility and the range of realistic variation the parameter can undergo.

Considering the severe limit now imposed on the cyclic fatigue reduction factor, a recalibration of  $C_f$ , following a full-scale investigation of the material fatigue behavior, hold hopes to turn the requirement from ruling to neglectable (Figure 3d) (Table 3). Conversely, an increment of the environmental reduction factor would be less effective, being the range of possible variation for the cyclic fatigue reduction coefficient larger than the one for the environmental reduction factor (Figure 3b) (Table 3). The same goes for the creep rupture reduction factor, as shown in Figure 3c and again in Table 3.

The prioritization of investigations into creep rupture and cyclic fatigue behavior is also suggested by mechanical considerations: it is well known how materials behave differently under a constantly applied load, rather than a cyclic one, and that failure under these two different conditions follows different mechanisms. Therefore, regardless of design requirement calibration, a deeper investigation into GFRP creep rupture and cyclic fatigue behavior, addressing the different nature of the phenomena, appears to be a priority.

A numerical example is presented, considering a variation of the creep rupture and cyclic fatigue reduction factor to ideal values ( $C_f = 0.35$ ,  $C_c = 0.35$ ). Furthermore, to limit the incidence of the minimum reinforcement requirement, the ratio  $M_r / M_{cr} = 1.2$  is adopted, consistent with the approach proposed by Gamble (2017). These assumptions result in a reduction of the required amount of reinforcement to 7.17 in<sup>2</sup> (4626 mm<sup>2</sup>). Operating on the environmental reduction factor would result in further gradational savings as shown in Figure 5.

A recalibration of the strength reduction factor would also prove effective, as long as the minimum reinforcement requirement is expressed as function of such a parameter (Eq. 4). The effect would however lack homogeneity, being creep rupture and fatigue requirements not affected, as shown in Figure 6.

As an alternative solution, to rationalize the incidence of creep rupture and cyclic fatigue on the required reinforcement, a recalibration of the load demand may be considered. Whereas the impact on creep may be limited [ $M_s^+ = 252$  kip-ft or 342 kN-m for SLS 1 load combination per CSA (2014)], fatigue design would be significantly affected [ $M_{s+f}^+ = 163$  kip-ft or 221 kN-m for FLS load combination per CSA (2014)], as shown in Figure 7.

In this scenario, creep rupture would govern over the other design parameters. Further understanding of GFRP-RC behavior under sustained loads would become a priority over cyclic fatigue characterization.

### SUMMARY AND CONCLUSIONS

A parametric analysis has been conducted on the equations governing the design of a large section GFRP-RC element, serving as pile cap for the short-spanned Halls River bridge. The relevance of cyclic fatigue and creep rupture as ruling design requirements has been pointed out and the influence of a set of four critical design factors on the reinforcement demand has been investigated. The separation of creep and fatigue reduction factors has been discussed in reason of the different load demand characterizing the requirements and the different material behavior under permanent and cyclic loading. An alternative approach to minimum reinforcement requirement has been considered as well.

The reinforcement demand proved to be sensible to the variation of creep reduction factor ( $C_c$ ) and fatigue reduction factor ( $C_f$ ) while the environmental reduction factor ( $C_e$ ) offers a narrower range of realistic variation. Conversely, the strength reduction factor ( $\Phi$ ) becomes influential only once fatigue and creep rupture are addressed and the approach to minimum reinforcement is made  $\Phi$ -dependent.

The definition of specific creep rupture reduction factor and cyclic fatigue reduction factor is proved to be a priority for the design optimization of large section GFRP-RC elements subject to severe cyclic and sustained loading. As an alternative solution, to rationalize the incidence of creep rupture and fatigue on the reinforcement demand, a recalibration of related load conditions, for example similar to CSA (2014), has been discussed.

Addressing creep rupture and cyclic fatigue demand may result in having the minimum required amount of reinforcement as the governing design requirement. A rational material-independent approach to the issue is discussed, based on Gamble (2017), and experimental validation is required.

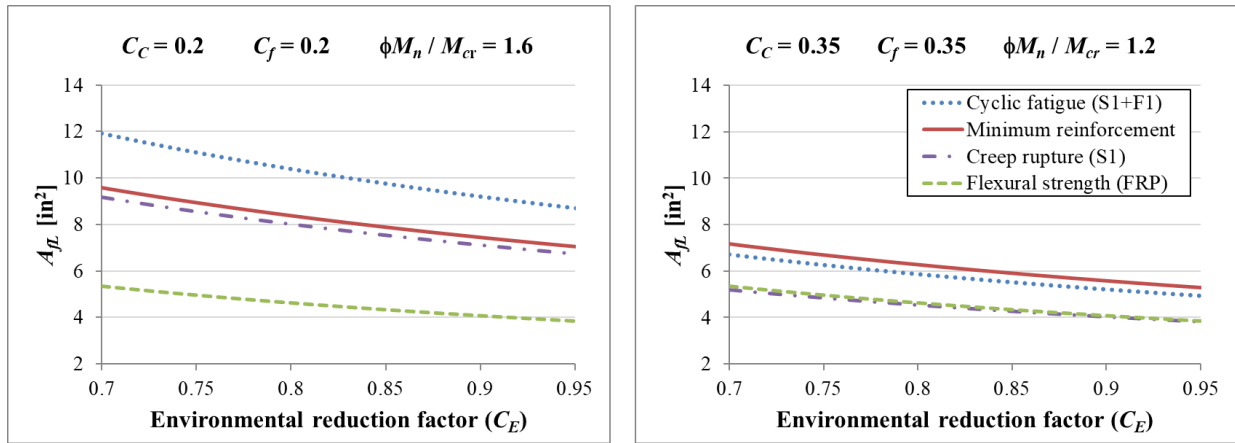


Figure 5 – Required area of reinforcement as a function of current and reduced design parameters, at varying environmental reduction factor ( $1 \text{ in}^2 = 645 \text{ mm}^2$ ).

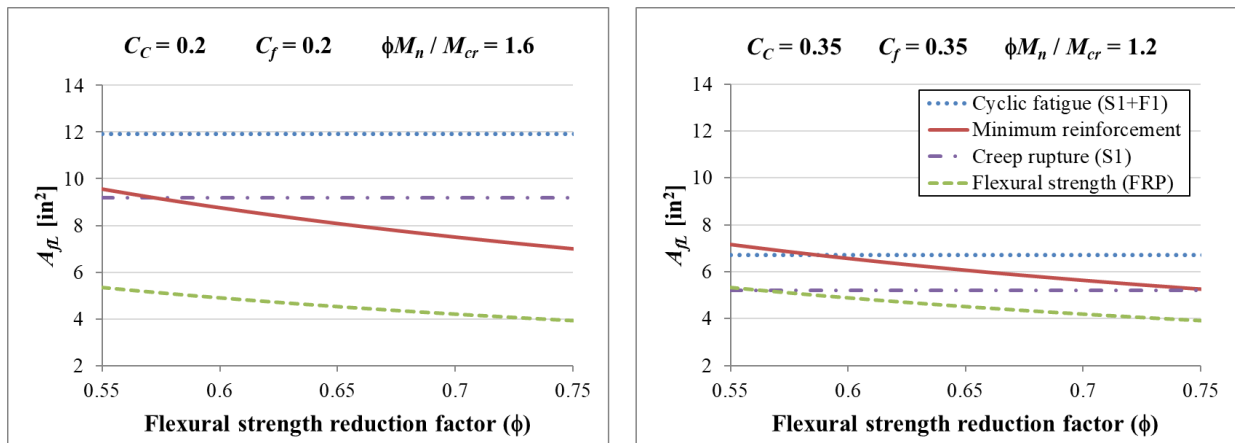


Figure 6 – Required area of reinforcement as a function of current and reduced design parameters, at varying strength reduction factor ( $1 \text{ in}^2 = 645 \text{ mm}^2$ ).

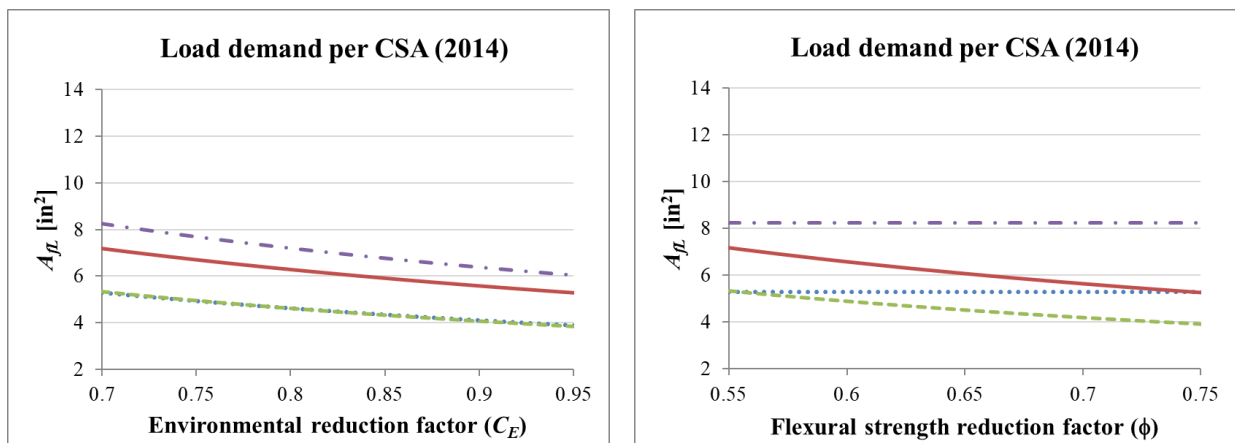


Figure 7 - Required area of reinforcement under CSA (2014) load combination as a function of current design parameters and reduced minimum reinforcement demand ( $1 \text{ in}^2 = 645 \text{ mm}^2$ ).

### ACKNOWLEDGEMENTS

The authors gratefully acknowledge the financial support from: (1) “Sustainable concrete using seawater, salt-contaminated aggregates, and non-corrosive reinforcement” Infravation, 31109806.005-SEACON. (2) “I/UCRC Center for the Integration of Composites into Infrastructure (CICI),” NSF, 1439543. And (3) Florida Department of Transportation (FDOT) for access to the Halls River Bridge design material.

### REFERENCES

- AASHTO. (2009). *AASHTO LRFD Bridge Design Guide Specifications for GFRP-Reinforced Concrete Bridge Decks and Traffic Railings*. Washington, DC: American Association of State Highway and Transportation Officials.
- AASHTO. (2014). *AASHTO LRFD Bridge Design Specifications 7th Edition*. Washington, DC: American Association of State Highway and Transportation Officials.
- ACI. (2014). *Building Code Requirements for Structural Concrete (ACI 318-14)*. Farmington Hills, MI: American Concrete Institute.
- ACI. (2015). *Guide for the Design and Construction of Structural Concrete Reinforced with Fiber-Reinforced Polymers (FRP) Bars (ACI 440.1R-15)*. Farmington Hills, MI: American Concrete Institute.
- ACI. (under ballot). *Building Code Requirements for GFRP-Reinforced Structural Concrete (ACI 440-xx)*. Farmington Hills, MI: American Concrete Institute.
- Benmokrane, B., Chaallal, O., & Masmoudi, R. (1996). Flexural Response of Concrete Beams Reinforced with FRP Reinforcing Bars. *ACI Structural Journal*, V. 93, No. 1, 46-55.
- CNR. (2007). *Guide for the Design and Construction of Concrete Structures Reinforced with Fiber-Reinforced Polymer Bars (CNR -DT 203/2006)*. Rome, Italy: National Research Council.
- CSA. (2014). *Canadian Highway bridge Design Code (CAN/CSA S6-14)*. Mississauga, Ontario, Canada: Canadian Standards Association.
- Hugo, J., Sova, M., & Cizinsky, J. (1993). Creep and Creep Damage of Glass Fibre Reinforced Polypropylene. *Composite Structures* 24, 233-244.
- Jawaheri, H. Z., & Nanni, A. (2013). Reliability Analysis of Concrete Beams Internally Reinforced with Fiber-Reinforced Polymer Bars. *ACI Structural Journal*, 1023-1031.
- JSCE. (2001). *Recommendation for the upgrading of concrete structures with use of continuous fiber sheet, Concrete engineering series nr 41*. Tokyo, Japan: Japanese Society of Civil Engineers.
- Nanni, A. (1993). Flexural Behavior and Design of RC Members Using FRP Reinforcement. *Journal of Structural Engineering* Vol. 119, Issue 11.
- Nanni, A. (1999). Composites: Coming on Strong. *Concrete Construction*, vol. 44, 120.
- Nanni, A., & Faza, S. (2002). Design and Construction of Concrete Reinforced with FRP Bars: An Emerging Technology.
- Wiederhorn, S. M., & Bolz, L. H. (1970). Stress Corrosion and Static Fatigue of Glass. *Journal of the American Ceramic Society*, Vol. 53, No. 10, 543-548.